Journal of Experimental Botany, Vol. 68, No. 20 pp. 5583–5597, 2017
doi:10.1093/jxb/erx350 Advance Access publication 16 October 2017
This paper is available online free of all access charges (see http://jxb.oxfordjournals.org/open_access.html for further details)

RESEARCH PAPER

Short-term thermal photosynthetic responses of C_4 grasses are independent of the biochemical subtype

Balasaheb V. Sonawane[1,†,*], Robert E. Sharwood[2], Susanne von Caemmerer[2], Spencer M. Whitney[2] and Oula Ghannoum[1]

[1] ARC Centre of Excellence for Translational Photosynthesis and Hawkesbury Institute for the Environment, Western Sydney University, Richmond NSW 2753, Australia
[2] ARC Centre of Excellence for Translational Photosynthesis and Research School of Biology, Australian National University, Canberra ACT 2601, Australia

* Correspondence: b.sonawane@wsu.edu
† Current address: School of Biological Sciences, Washington State University, Pullman WA 99164-4236, USA

Received 27 June 2017; Editorial decision 8 September 2017; Accepted 14 September 2017

Editor: Christine Raines, University of Essex

Abstract

C_4 photosynthesis evolved independently many times, resulting in multiple biochemical pathways; however, little is known about how these different pathways respond to temperature. We investigated the photosynthetic responses of eight C_4 grasses belonging to three biochemical subtypes (NADP-ME, PEP-CK, and NAD-ME) to four leaf temperatures (18, 25, 32, and 40 °C). We also explored whether the biochemical subtype influences the thermal responses of (i) *in vitro* PEPC (V_{pmax}) and Rubisco (V_{cmax}) maximal activities, (ii) initial slope (IS) and CO_2-saturated rate (CSR) derived from the A-C_i curves, and (iii) CO_2 leakage out of the bundle sheath estimated from carbon isotope discrimination. We focussed on leakiness and the two carboxylases because they determine the coordination of the CO_2-concentrating mechanism and are important for parameterizing the semi-mechanistic C_4 photosynthesis model. We found that the thermal responses of V_{pmax} and V_{cmax}, IS, CSR, and leakiness varied among the C_4 species independently of the biochemical subtype. No correlation was observed between V_{pmax} and IS or between V_{cmax} and CSR; while the ratios V_{pmax}/V_{cmax} and IS/CSR did not correlate with leakiness among the C_4 grasses. Determining mesophyll and bundle sheath conductances in diverse C_4 grasses is required to further elucidate how C_4 photosynthesis responds to temperature.

Key words: Biochemical subtypes, C_4 photosynthesis, CO_2 concentrating mechanism, thermal responses.

Introduction

Understanding how photosynthesis responds to temperature is critical to our ability to predict the responses of natural and cropping ecosystems to climate change. Modelling the photosynthetic responses of C_3 plants to temperature is a routine task where we have a growing appreciation of the natural variation in the underlying mechanisms, such as the temperature dependence of mesophyll conductance (g_m) and the kinetics of the CO_2-fixing enzyme ribulose 1,5-bisphosphate carboxylase/oxygenase (Rubisco) (Farquhar *et al.*, 2001; Bernacchi *et al.*, 2013; Walker *et al.*, 2013; von Caemmerer and Evans, 2015; Sharwood *et al.*, 2016*a*). Unlike its C_3 counterpart, the semi-mechanistic C_4 photosynthesis model (Farquhar, 1983; von Caemmerer, 2000) has not been comprehensively tested across a wide range of species and temperatures. Addressing

this gap is critical given that C_4 plants include some of the world's most important food, feed, and biofuel crops (e.g. maize, sorghum, and sugarcane), dominate the understory of warm-climate grasslands and savannas (Ehleringer and Monson, 1993; Brown, 1999; Sage *et al.*, 2013), and account for 20–25% of terrestrial productivity (Lloyd and Farquhar, 1994).

C_4 photosynthesis has evolved independently many times, resulting in multiple biochemical pathways named after the primary C_4-acid decarboxylase enzyme found in the bundle sheath cells (BSCs), which are NADP-malic enzyme (-ME), NAD-ME, and phosphoenolpyruvate carboxykinase (PEP-CK) (Hatch 1987). Although PEP-CK operates as a secondary decarboxylase in many C_4 species (Leegood and Walker, 2003; Furbank, 2011; Sharwood *et al.*, 2014; Wang *et al.*, 2014), the primary decarboxylase is generally associated with a suite of anatomical, biochemical, and physiological features (Gutierrez *et al.*, 1974; Hattersley, 1992; Kanai and Edwards, 1999; Ghannoum *et al.*, 2011). The grass family includes species from all biochemical subtypes, but little is known about how these different pathways respond to temperature.

C_4 photosynthesis is characterized by the operation of a CO_2-concentrating mechanism (CCM) comprising a C_4 cycle that fixes atmospheric CO_2 into a C_4 acid in mesophyll cells (MCs) that is then transported to, and decarboxylated in, BSCs where Rubisco and the C_3 cycle are localized (Hatch, 1987). The C_4 cycle is faster than the C_3 cycle, resulting in elevated CO_2 in the BSCs and thus minimizing photorespiration and maximizing CO_2 assimilation rates at low intercellular CO_2 (C_i) (Hatch, 1987; Kanai and Edwards, 1999). Some CO_2 leaks out of the BSCs into the surrounding MCs, costing additional ATP that is required for the phosphorylation of phospenolpyruvate (PEP) in the MCs (Hatch, 1987).

Leakiness (ϕ) describes the efficiency of C_4 photosynthesis and is defined as the rate of CO_2 leakage out of the BSCs as a fraction of the rate of PEP carboxylation or C_4 cycle rate (V_p) (Farquhar, 1983). According to the C_4 model, CO_2 leakage (L) depends on the BSC wall conductance to CO_2 (g_{bs}) and the gradient between the CO_2 concentration in the BSCs (C_{bs}) and MCs (C_m), such that $L=g_{bs}(C_{bs}–C_m)$. In turn, the BSC–MC CO_2 gradient depends on the balance between the activity of the C_4 (e.g. PEP carboxylase, PEPC) and C_3 (e.g. Rubisco) cycles (Henderson *et al.*, 1992; von Caemmerer, 2000). The C_4 photosynthesis model stipulates that the initial slope of the A-C_i curve (IS) depends on the maximal PEPC activity (V_{pmax}) while the CO_2-saturated rate (CSR) depends on maximal Rubisco activity (V_{cmax}), in addition to other factors (von Caemmerer, 2000). Consequently, the thermal responses of V_{pmax} and V_{cmax} are expected to influence the thermal response of both IS and CSR as well as the BSC–MC CO_2 gradient, and hence leakiness. Therefore, in this study we asked whether the thermal responses of these key parameters (V_{pmax}, V_{cmax}, IS, CSR, and ϕ) depend on the biochemical subtype of the C_4 species.

In a recent study, Sharwood *et al.* (2016*a*) showed that the declining response of Rubisco's *in vitro* CO_2/O_2 specificity ($S_{c/o}$) with increasing temperature was more pronounced for NAD-ME relative to PEP-CK and NADP-ME species. Given that the CSR of C_4 leaves depends strongly on Rubisco and its catalytic properties, we predict that, relative to the other two subtypes, V_{cmax} of NAD-ME species may increase less with temperature, with possible consequences on V_{pmax}/V_{cmax} and ϕ. These predictions remain untested, especially in that thermal responses of V_{pmax} have been less widely studied than V_{cmax} (Tieszen and Sigurdson, 1973; Pittermann and Sage, 2000; Sage, 2002; Boyd *et al.*, 2015; Sharwood *et al.*, 2016*a*).

In an earlier study, high leaf temperature was found to increase O_2 uptake in NAD-ME but not NADP-ME species, pointing to increased Mehler reaction and/or Rubisco oxygenation at higher temperature in NAD-ME species (Siebke *et al.*, 2003). Higher Rubisco oxygenation may be symptomatic of a less favorable CO_2/O_2 concentration ratio in the BSCs, which is corroborated by the less relaxed Rubisco affinity for CO_2 (higher $K_{m(CO2)}$) in NAD-ME relative to NADP-ME subtypes (Sharwood *et al.*, 2016*a*). The suberin lamella lining the BSC walls of NADP-ME and PEP-CK grasses may reduce g_{bs}, which could impact C_{bs} (Hatch, 1987; von Caemmerer and Furbank, 2003). Consequently, we predict that C_{bs} and hence leakiness may be affected differently by temperature depending on the C_4 subtypes. Previous measurements revealed a slight decrease in leakiness in response to increasing temperature between 21 and 35 °C for the C_4 monocot *Sorghum bicolor* (Henderson *et al.*, 1992). To our knowledge, the thermal response of leakiness has not yet been compared in C_4 grasses with different biochemical subtypes.

The temperature dependence of key parameters of the C_4 photosynthesis model has primarily been determined for a few representative species, such as maize and *Setaria* (Henderson *et al.*, 1992; Chen *et al.*, 1994; Massad *et al.*, 2007; Boyd *et al.*, 2015). In addition, parameterization can be done *in vivo* (derived from gas exchange) or *in vitro* (derived from enzyme assays), but comparisons between these two parameterization methods remains unexplored for different C_4 species and temperatures. Relationships between ϕ and the ratio of *in vivo* (IS/CSR) or *in vitro* (V_{pmax}/V_{cmax}) activities of C_4 and C_3 carboxylases have been demonstrated for single species under different growth environments (Ranjith *et al.*, 1995; Saliendra *et al.*, 1996; Meinzer and Zhu, 1998; Gong *et al.*, 2017). However, such relationships have rarely been explored for diverse C_4 grasses at different temperatures. Addressing these knowledge gaps is critical to our ability to interpret gas exchange data and relate them to underlying biochemistry, as has been done for C_3 plants (von Caemmerer and Farquhar, 1981; Hudson *et al.*, 1992; Bernacchi *et al.*, 2001).

Consequently, in this study we measured the photosynthetic thermal responses of eight diverse C_4 grasses belonging to the three biochemical subtypes. We aimed at determining whether the C_4 biochemical subtype influences the thermal responses of (i) *in vitro* PEPC (V_{pmax}) and Rubisco (V_{cmax}) maximal activities, (ii) initial slope (IS) and CO_2-saturated rate (CSR) derived from the A-C_i curves, and (iii) CO_2 leakage out of the bundle sheath as estimated from carbon isotope discrimination. Our results showed that the thermal photosynthetic responses varied among the C_4 species independently of the biochemical subtype. We also observed that

the ratios of IS/CS and V_{pmax}/V_{cmax} were uncorrelated with each other or with leakiness when determined for a range of C_4 species. Finally, we derived constants for thermal dependency that can be incorporated in the C_4 photosynthesis model.

Material and methods

Plant culture

The experiment was conducted in a naturally lit glasshouse chamber (5 m^3) with a mean noon photosynthetic photon flux density (PPFD) of 1230 ± 22 µmol quanta m^{-2} s^{-2} (±SE) and a 10-h photoperiod (see Supplementary Fig. S1 at *JXB* online). The air temperature inside the glasshouse compartment was regulated and day/night temperatures averaged 28/22 °C. Relative humidity was monitored and ranged between 60–80% during the day. Grass seeds (Table 1) were obtained from the Australian Plant Genetic Resources Information System, Australia. Seeds were sown in germination trays containing a common germination mixture. Seedlings at 3–4 weeks old were transplanted into the experimental pots (2 l) containing Osmocote® Professional – Seed Raising & Cutting Mix (Scotts; www.scottsaustralia.com.au). Nutrients were supplied through the addition of Osmocote® Plus Trace Element: Total All Purpose (N:P:K=19.4:1.6:5) (Scotts) and periodic watering with soluble Aquasol (N:P:K=23.3:3.95:14) (Yates; www.yates.com.au/). For each species there were eight pots, each of which contained a single plant. Pots were well-watered and regularly rotated within the glasshouse chamber.

Leaf gas exchange measurements

Leaf gas exchange measurements were carried out using a portable open photosynthesis system (LI-6400XT, LI-COR, Lincoln, USA). Measurements were conducted between 10.00 h and 14.00 h, 7–8 weeks after transplanting, on the last fully expanded leaf (LFEL) attached on the main stem. Prior to gas exchange measurements, plants were moved to another chamber where air temperature could be changed separately. Measurements were made at leaf temperatures of 18, 25, 34, and 40 °C by using the internal heating system of the photosynthesis unit in conjunction with the glasshouse chamber heating system, whilst maintaining a relatively constant humidity inside the leaf chamber. Prior to measurements, each leaf was allowed to reach a steady state of CO_2 uptake at ambient CO_2 (Reference=400 µl l^{-1}), PPFD of 1800 µmol m^{-2} s^{-1}, and relative humidity of 50–70%. A steady-state measurement was taken at each of the four leaf temperatures, and this was followed by measuring the responses of CO_2 assimilation rate (A) to step increases of intercellular CO_2 (C_i) by raising the LI-6400XT leaf chamber [CO_2] in 10 steps (i.e. 50, 100, 150, 200, 250, 325, 400, 650, 1200, and 1500 µl l^{-1}) with 2 and 3 min as the minimum and maximum waiting times during each step change, respectively. For dark respiration, light in the LI-6400XT leaf chamber was switched off for 20 min before measurements were made. There were three or four biological replicates, i.e. plants per species. The initial slope (IS) of each A-C_i curve was estimated by fitting a linear model to the initial 3–4 linear data points such that maximum C_i was about 55 µl l^{-1} at all leaf temperatures. The maximum CO_2-saturated rate of each A-C_i curve at each leaf temperature was considered as the CO_2-saturated rate (CSR).

Table 1. *List of C_4 grasses used in the current study.*

C_4 Subtype	C_4 tribe	Species
NADP-ME	Paniceae	*Cenchrus ciliaris*
	Andropogoneae	*Sorghum bicolor*
		Zea mays
PEP-CK	Paniceae	*Eriochloa meyeriana*
	Chloridoideae	*Megathyrsus maximus*
		Chloris gayana
NAD-ME	Paniceae	*Panicum coloratum*
	Chloridoideae	*Leptochloa fusca*

Calculation of photosynthetic carbon isotope discrimination, leakiness, and C_4 cycle rate

Bundle-sheath leakiness was determined by measuring real-time $^{13}CO_2/^{12}CO_2$ carbon isotope discrimination using a LI-6400XT attached to a tunable diode laser (TDL, model TGA100, Campbell Scientific, Inc., Logan, Utah, USA) under similar conditions to the steady-state measurements. For estimation of TDL precision, we used the $\delta^{13}C$ value of the LI-6400XT reference gas for *S. bicolor*. The mean SD of repeated measurements for $\delta^{13}C$ were 0.24, 0.14, 0.20, and 0.28‰ at 18, 25, 32, and 40 °C, respectively, with an overall SD of 0.21‰. Photosynthetic carbon isotope discrimination (Δ) was calculated according to Evans *et al.* (1986):

$$\Delta = \frac{\xi \cdot (\delta_o - \delta_e)}{1 + \delta_o - \xi \cdot (\delta_o - \delta_e)} \quad (1)$$

$$\xi = \frac{C_e}{C_e - C_o} \quad (2)$$

where δ_e, δ_o, C_e, and C_o are the $\delta^{13}C$ (δ) and CO_2 mol fraction (C) measured with the TDL of the air entering (e) and leaving (o) the leaf chamber. Leakiness (ϕ) was calculated using the model of Farquhar (1983) as modified by Pengelly *et al* (2010) and Pengelly *et al* (2012). The slightly modified equation used here is:

$$\phi = \frac{\left(\frac{1-t}{1+t}\right)\cdot\Delta - \frac{a'}{1+t} - \left(a_i - b_4'\right)\cdot\frac{A}{g_m \cdot C_a} - \left(b_4' - \frac{a'}{1+t}\right)\cdot\frac{C_i}{C_a}}{(b_3' - s)\cdot\left(\frac{C_i}{C_a} - \frac{A}{C_a \cdot g_m}\right)} \quad (3)$$

where Δ is the photosynthetic carbon isotope discrimination measured by the TDL. a_i is the fractionation factor associated with the dissolution of CO_2 and its diffusion through water. Here, we assume that s=a_i. The term t, which represents ternary effects of transpiration rate on the carbon isotope discrimination during CO_2 assimilation, is defined according to Farquhar and Cernusak (2012) as:

$$t = \frac{(1+a')\cdot E}{2g^{t}_{ac}} \quad (4)$$

where E is the transpiration rate and g^{t}_{ac} is the total conductance to CO_2 diffusion including boundary layer and stomatal conductance (von Caemmerer and Farquhar, 1981).

The combined fractionation factor through the leaf boundary layer and stomata is denoted by a':

$$a' = \frac{a_b\cdot(C_a - C_{ls}) + a\cdot(C_{ls} - C_i)}{C_a - C_i} \quad (5)$$

where: C_a, C_i, and C_{ls} are the ambient, intercellular, and leaf surface CO_2 partial pressures, respectively; a_b (2.9‰) is the fractionation occurring through diffusion in the boundary layer; s (1.8‰) is the fractionation during leakage of CO_2 out of the bundle sheath; and a (4.4‰) is the fractionation due to diffusion in air (Evans *et al.*, 1986).

$$b_3' = b_3 - e\cdot\left(\frac{R_d}{A+R_d} - \frac{0.5\cdot R_d}{A+0.5\cdot R_d}\right) - f\cdot\frac{\Gamma^*}{C_s} \quad (6)$$

and

$$b_4' = b_4 - e\cdot\frac{0.5\cdot R_d}{(A+0.5\cdot R_d)} \quad (7)$$

where: b_3 is the fractionation by Rubisco (30‰); b_4 is the combined fractionation of the conversion of CO_2 to HCO_3^- and PEP carboxylation (–5.74‰ at 25 °C); f is the fraction associated with photorespiration; Γ* is the CO_2 partial pressure where rate of photorespiratory CO_2 release balances the rate of carboxylation; and C_s is the CO_2 partial pressure in the BSC. The fractionation factor e associated with respiration was calculated from the difference between $\delta^{13}C$ in the CO_2 cylinder used during experiments (–5.6‰) and that in the atmosphere under growth conditions (–8‰) (Tazoe *et al.*, 2008). A and R_d denote the CO_2 assimilation rate and daytime respiration, respectively; R_d was assumed equal to the measured dark respiration (Atkin *et al.*, 1997). We considered mesophyll conductance (g_m) to be 1.78 mol m^{-2} s^{-1} at 30 °C (Barbour *et al.*, 2016; Ubierna *et al.*, 2017). The temperature dependency of g_m was accounted for by using the Arrhenius function:

$$g_m = g_{m25}\cdot e^{E_a\cdot\frac{T_k - 298.15}{298.15\cdot R\cdot T_k}} \quad (8)$$

where T_k is the leaf temperature in K; g_{m25} is the mesophyll conductance at 25 °C; E_a is the activation energy, taken as 40.6 kJ mol^{-1} (the value for for *Zea mays*) (Ubierna *et al.*, 2017); and R is the universal gas constant (0.008314 kJ K^{-1}). In this study, leaf gas exchange was measured at high light and it was assumed that $f\frac{\Gamma^*}{C_s} = 0$ (Pengelly *et al.*, 2010, 2012; Ubierna *et al.*, 2013; von Caemmerer *et al.*, 2014).

We used ϕ, A and R_d to calculate the C_4 cycle rate (V_p), assuming that Rubisco oxygenation approximated to zero, i.e. $V_o \approx 0$ (Pengelly *et al.*, 2012).

$$V_p = \frac{A + 0.5R_d}{1-\phi} \quad (9)$$

Determination of Rubisco and soluble protein contents

Following gas exchange measurements, replicate leaf discs were cut and rapidly frozen in liquid nitrogen and then stored at –80 °C until analysis. Each leaf disc was extracted in 0.8 ml of ice-cold extraction buffer [50 mM EPPS-NaOH (pH 7.8), 5 mM DTT, 5 mM $MgCl_2$, 1 mM EDTA, 10 µl protease inhibitor cocktail (Sigma), 1% (w/v) polyvinyl polypyrrolidone] using a 2-ml Tenbroeck glass homogenizer kept on ice. The extract was centrifuged at 15 000 rpm for 1 min and the supernatant was used for enzyme activity (see below), Rubisco content, and soluble protein assays. For Rubisco content, subsamples were activated in buffer [50 mM EPPS (pH 8.0), 10 mM $MgCl_2$, 2 mM EDTA, 20 mM $NaHCO_3$], and content was estimated by the irreversible binding of [^{14}C]-CABP to the fully carbamylated enzyme (Sharwood *et al.*, 2008). Extractable soluble proteins were measured using the Pierce Coomassie Plus (Bradford) protein assay kit (Thermo scientific, Rockford, USA).

In vitro *thermal response of Rubisco and PEPC activities*

Enzymatic assays were done for Rubisco and PEPC at 18, 25, 34 and 40 °C. To achieve the target temperatures, cuvettes with assay buffer were kept in incubators for 20 min (18 °C), 10 min (25 °C), 10 min (34 °C), and 5 min (40 °C). The maximal *in vitro* activities of Rubisco (V_{cmax}) and PEPC (V_{pmax}) were measured spectrophotometrically as described previously (Jenkins *et al.*, 1987; Ashton *et al.*, 1990; Sharwood *et al.*, 2008, 2014, 2016*b*; Pengelly *et al.*, 2010). Briefly, V_{cmax} was measured in assay buffer [50 mM EPPS-NaOH (pH 8), 10 mM $MgCl_2$, 0.5 mM EDTA, 1 mM ATP, 5 mM phosphocreatine, 20 mM $NaHCO_3$, 0.2 mM NADH, 50 U creatine phosphokinase, 0.2 mg carbonic anhydrase, 50 U 3-phosphoglycerate kinase, 40 U glyceraldehyde-3-phosphate dehydrogenase, 113 U triose-phosphate isomerase, 39 U glycerol-3-phosphate dehydrogenase] and the reaction was initiated by the addition of 0.22 mM ribulose-1, 5-bisphosphate (RuBP). V_{pmax} was measured in assay buffer [50 mM EPPS-NaOH (pH 8.0), 0.5 mM EDTA, 10 mM $MgCl_2$, 0.2 mM NADH, 5 mM glucose-6-phosphate, 0.2 mM NADH, 1 mM $NaHCO_3$, 1 U MDH] after the addition of 4 mM PEP. Maximal activities of Rubisco and PEPC were calculated by monitoring the decrease of NADH absorbance at 340 nm using a UV-VIS spectrophotometer (model 8453, Agilent Technologies Australia, Mulgrave, Victoria).

Temperature dependency

The temperature response of A, CSR, IS, V_{pmax}, and V_{cmax} were fitted in the R software (R Development Core Team, 2015) using two different equations, as follows. A modified form of the Arrhenius equation was used to fit the temperature

dependence, which yields a peak function (Harley *et al.*, 1992; Crous *et al.*, 2013), and is given by the following equation:

$$f(T_k) = k_{25} \cdot e^{\left[\frac{E_a \cdot (T_k - 298)}{298 \cdot T_k \cdot R}\right]} \cdot \left[\frac{1 + e^{\left(\frac{298 \cdot \Delta S - H_d}{298 \cdot R}\right)}}{1 + e^{\left(\frac{T_k \cdot \Delta S - H_d}{T_k \cdot R}\right)}}\right] \quad (10)$$

where, T_k is the measurement temperature (either leaf or assay buffer) in K; E_a is the activation energy (kJ mol^{-1}) and represents the expansion for the initial part of the temperature response curve; k_{25} is the parameter at 25 °C; H_d is the deactivation energy (kJ mol^{-1}); R is the universal gas constant; and ΔS (kJ mol^{-1} K^{-1}) is the entropy term, which describes the peak part of the curve. H_d and ΔS together describe the rate of decrease in the function above the optimum. To avoid over-parameterization, the H_d of all parameters was set as constant (200 kJ mol^{-1}) for model fitting, as has been done previously (Medlyn *et al.*, 2002; Crous *et al.*, 2013).

The outputs from the modified Arrhenius and the June *et al.* (2004) equations are compared in Supplementary Fig. S2. The modified form of the Arrhenius equation over-estimates the optimum parameter rate, P_{opt}, at the temperature optimum, T_{opt}. Consequently, T_{opt} and P_{opt} were derived by following the June *et al.* (2004) equation:

$$f(T) = P_{opt} \cdot e^{-\left(\frac{T - T_{opt}}{\Omega}\right)^2} \quad (11)$$

where T is the measurement temperature (either leaf or assay buffer) of parameter P in °C; P_{opt} is the optimum parameter rate at the optimum temperature, T_{opt}; and Ω is the difference in temperature from T_{opt} at which the parameter falls to e^{-1} (0.37) of its value at T_{opt}. A smaller value of Ω means a narrower peak. This equation effectively assumes that the reversible processes are symmetrical around the optimum temperature.

Statistical analyses

The statistical design included species, subtypes, and leaf temperature as factors. Due to the limited number of species used, the statistical analyses could not incorporate phylogenetic or evolutionary effects. Gas exchange measurements and enzyme activity measurements were performed on three or four replicates at each temperature. The coefficients derived by fitting equations (10) and (11) for each parameter were used to test for differences between the thermal responses of species and subtypes. The effect of species was compared using a linear model with type-II ANOVA. The effect of subtype was compared using a linear mixed-effect model using the lme4 package (https://rdrr.io/cran/lme4/) in R (R Development CoreTeam, 2015). Significance tests were performed using type-II ANOVA. Coefficient means were ranked using *post hoc* Tukey tests.

Recent studies have highlighted the flexibility of the decarboxylases; in particular, the expression of PEP-CK activity in NADP-ME subtypes (Wingler *et al.*, 1999; Furbank, 2011; Bellasio and Griffiths, 2014). Except for a relatively high activity in *Z. mays* (one-third of total decarboxylase activity), PEP-CK activity for most NADP-ME subtypes including those used in the current study does not exceed 5–25% of the total decarboxylase activity (see Supplementary Fig. S3). In addition, among the three species in the NADP-ME subtype, two are highly domesticated (*S. bicolor* and *Z. mays*), and *Z. mays* and *Cenchrus ciliaris* had appreciable secondary PEP-CK activity. However, the three NADP-ME species did not separate according to their known PEP-CK activity or domestication for the parameters collected (Supplementary Fig. S3). Consequently, for the purposes of the current study, it was valid to analyse the NADP-ME species as a single group rather than as one made up of multiple subgroups.

Results

Leaf gas exchange at 25 °C

Leaf gas exchange parameters were measured at ambient CO_2 and near-saturating light intensity for all the C_4 grasses concurrently with stable carbon isotope discrimination. At 25 °C, net CO_2 assimilation rate (A), stomatal conductance (g_s), the ratio of internal to atmospheric CO_2 partial pressure (C_i/C_a), dark respiration (R_d), and photosynthetic carbon isotope discrimination (Δ) all varied significantly among the species (P<0.05; Fig. 1, Supplementary Table S1). Only A varied significantly (P<0.05) according to the C_4 subtype, with NAD-ME species having lower A relative to NADP-ME and PEP-CK species. Photosynthetic carbon isotope discrimination was lowest in *Megathyrsus maximus* and *Z. mays*, and highest in *C. ciliaris*, *Chloris gayana*, and *Leptochloa fusca*.

Temperature response of leaf gas exchange

The initial slope (IS) and CO_2-saturated rate (CSR) of photosynthetic response to intercellular CO_2 partial pressure (from A-C_i curves) were estimated at four temperatures (see Supplementary Fig. S4). At 25 °C, IS, CSR, and IS/CSR varied significantly with species but not with subtypes. *Zea mays* and *L. fusca* had the highest IS and IS/CSR, while *M. maximus* had the lowest CSR relative to the other C_4 species (Fig. 2, Supplementary Table S2).

Rubisco and PEPC measurements at 25 °C

Maximal activities of PEPC (V_{pmax}) and Rubisco (V_{cmax}) were measured on the same leaves used for gas exchange. At 25 °C, V_{cmax} and V_{pmax} were highest in the two NADP-ME subtypes *S. bicolor* and *Z. mays*. V_{pmax} and V_{pmax}/V_{cmax} were lowest in the two NAD-ME subtypes along with *M. maximus* (PEP-CK) relative to the other species (Fig. 3, Supplementary Table S2). In line with earlier studies, we obtained an average extraction yield of 80% for V_{cmax} (maximal CO_2 assimilation/Rubisco activity) for wild C_4 grasses (Meinzer and Zhu, 1998; Kingston-Smith *et al.*, 1999; Crafts-Brandner and Salvucci, 2002; Dwyer *et al.*, 2007).

Leaf Rubisco content varied among the species (3.8–7.8 μmol sites m^{-2}), constituting about 6% of the soluble

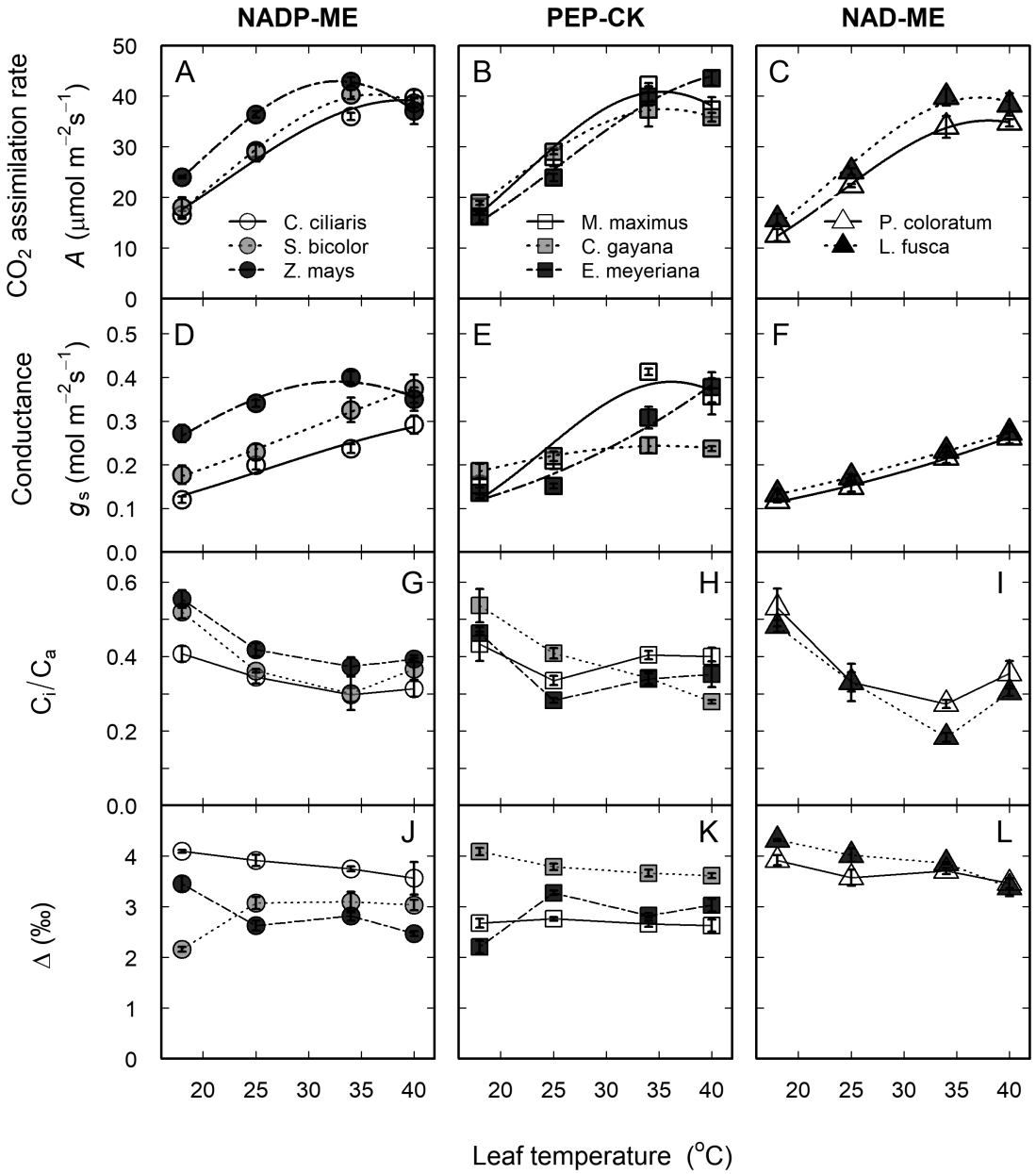

Fig. 1. Thermal responses of leaf gas exchange and photosynthetic carbon isotope discrimination in eight C_4 grasses. (A–C) CO_2 assimilation rate, A, (D–F) stomatal conductance, g_s, (G–I) ratio of intercellular to ambient CO_2, C_i/C_a, and (J–L) photosynthetic carbon isotope discrimination, Δ, as a function of leaf temperature for the C_4 subtypes NADP-ME, PEP-CK, and NAD-ME (as indicated). The grasses were grown in a common glasshouse. Data in (A–F) were fitted according to June *et al.* (2004) and the derived constants are shown in Table 2. Leaves were measured at 1800 μmol m^{-2} s^{-1} PPFD and 400 μl l^{-1} CO_2. Values are means of 3–4 replicates ±SE.

protein fraction (Supplementary Table S3). Among all the species, Rubisco and soluble protein contents were highest in *Z. mays* and *Panicum coloratum* and lowest in *C. ciliaris*, *Eriochloa meyeriana*, and *L. fusca*. Rubisco activation measured at 25 °C tended to be higher in NADP-ME (69%) compared to PEP-CK (53%) and NAD-ME (54%) subtypes.

Thermal responses of photosynthetic parameters

The short-term thermal responses of A, IS, CSR, V_{pmax}, and V_{cmax} were well characterized by the modified Arrhenius and June *et al.* (2004) equations (equations 10 and 11, Supplementary Figs S2 and S5–S8). No subtype effect was observed for the activation energy (E_a), entropy factor (ΔS), parameter at 25 °C (k_{25}), the optimum parameter (P_{opt}) at the optimum temperature (T_{opt}), or the width of curvature around T_{opt} (Ω) derived for IS, CSR, V_{pmax}, and V_{cmax} (Table 2).

For CO_2 assimilation rate, the range of variation observed for T_{opt} (33–43 °C), E_a (34–54 kJ mol^{-1}), and Ω (18–24 °C) was not significantly different among all the species (Fig. 1A–C, Table 2). E_a was significantly lower (P<0.05) in NADP-ME subtypes (37 kJ mol^{-1}) relative to NAD-ME (52 kJ mol^{-1}). Conversely, k_{25} tended to higher (P=0.1) in NADP-ME subtypes relative to NAD-ME. For CSR, *C. ciliaris* had the highest P_{opt}, T_{opt}, and Ω, while *P. coloratum* and *M. maximus* had the lowest P_{opt}, and *Z. mays* and *P. coloratum* had the

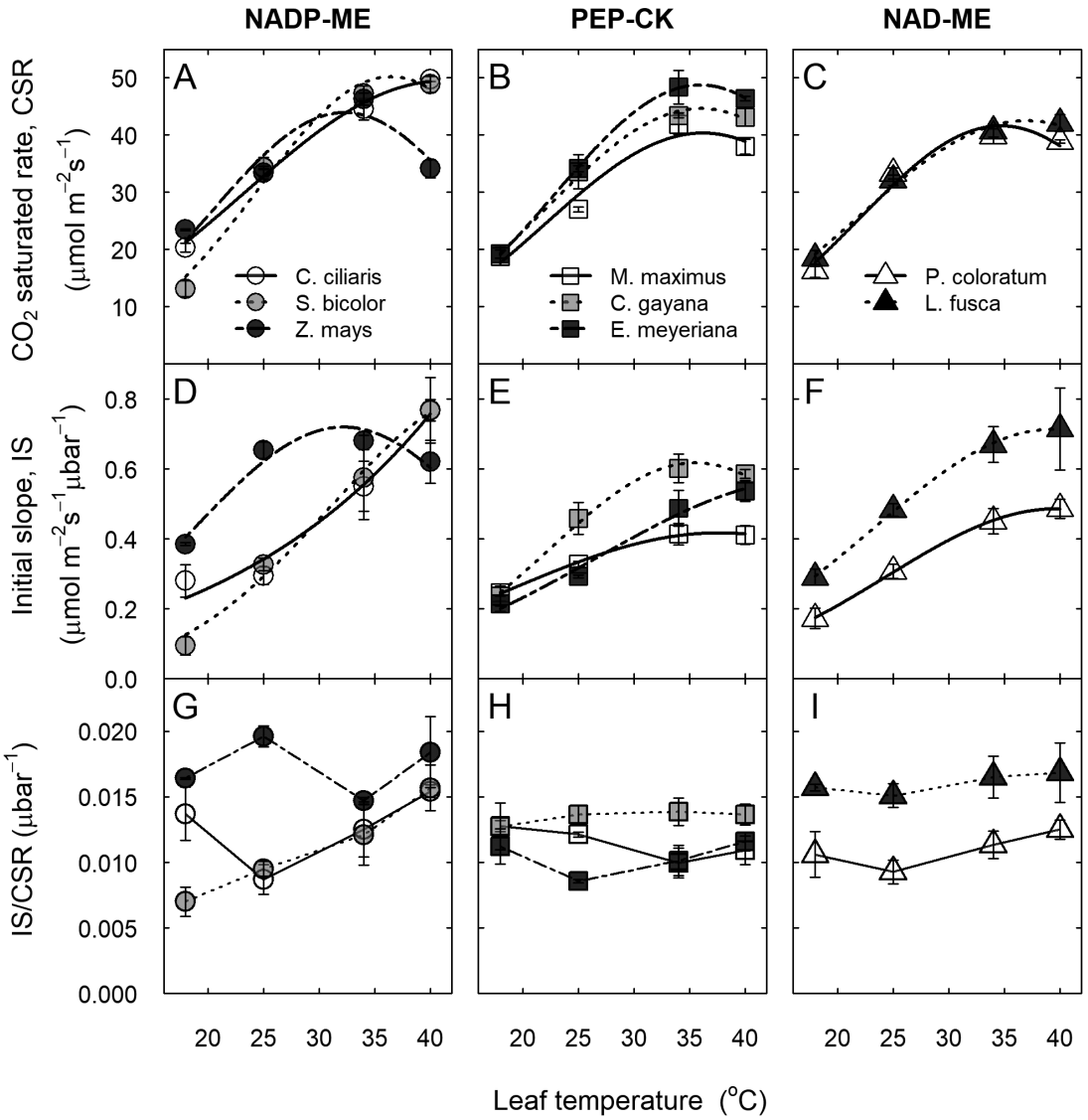

Fig. 2. Thermal responses of the CO_2-saturated rate (CSR) and the initial slope of the *A*-C_i curve (IS) in eight C_4 grasses. (A–C) CO_2-saturated rate, CSR, (D–F) initial slope of the CO_2 response curve, IS, and (G–I) the IS/CSR ratio as a function of leaf temperature for the C_4 subtypes NADP-ME, PEP-CK, and NAD-ME (as indicated). Data in (A–F) were fitted according to June *et al.* (2004) and the derived parameters are shown in Table 2. Leaves were measured at 1800 μmol m^{-2} s^{-1} PPFD. Values are means of 3–4 replicates ±SE

lowest T_{opt}. For IS, *C. ciliaris* had the highest T_{opt}, P_{opt}, and Ω, while E_a was highest in *S. bicolor* and lowest in *Z. mays* and *M. maximus* relative to the other species (Fig. 2, Table 2). Overall, the ratio IS/CSR was not affected by leaf temperature, except in *S. bicolor* where IS/CSR increased with temperature (Fig. 2, Supplementary Table S2).

For the temperature response of *in vitro* V_{cmax}, no parameter varied significantly according to the biochemical subtype, while E_a, k_{25}, and P_{opt} varied among all the species (Table 2). Rubisco E_a was highest in *L. fusca* (58 kJ mol^{-1}) and lowest in *S. bicolor* (36 kJ mol^{-1}), while Rubisco k_{25} and P_{opt} were highest in *S. bicolor* and *Z. mays* and lowest in *C. ciliaris* (Fig. 3A–C, Table 2).

All parameters describing the thermal response of *in vitro* V_{pmax} varied significantly among all the species. In addition, P_{opt} and k_{25} tended to be lowest (P<0.07) in NAD-ME, intermediate in PEP-CK, and highest in NADP-ME subtypes (Fig. 3D–F, Table 2). Overall, the ratio IS/CSR was unaffected by leaf temperature (Fig. 3, Supplementary Table S2).

Photosynthetic carbon isotope discrimination and bundle sheath leakiness

Photosynthetic carbon isotope discrimination (Δ) was unchanged between 25 and 40 °C and increased significantly at 18 °C for most of the species, except in *S. bicolor* and *E. meyeriana* where it decreased at 18 °C (Fig. 1J–L Supplementary Table S1). Overall, the NAD-ME subtypes showed higher Δ compared to NADP-ME and PEP-CK. Leakiness (ϕ) was higher at the two lowest temperatures (18 and 25 °C) relative to the two highest temperatures (34 and 40 °C), with ϕ at 40 °C being similar among all the species (Fig. 4A–C, Supplementary Table S1). *Sorghum bicolor*, *M. maximus*, and *E. meyeriana* had lower ϕ relative to the other species at

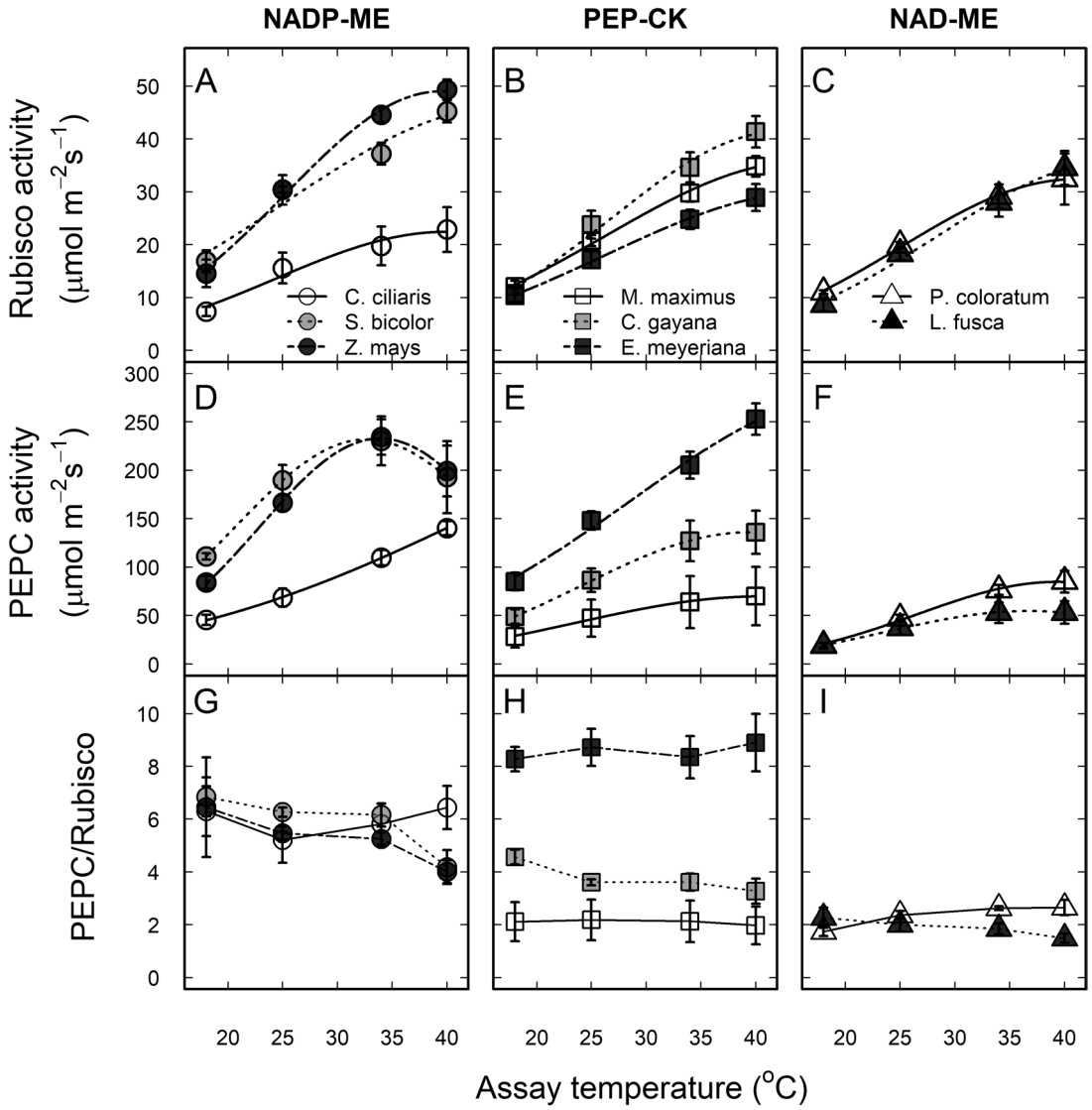

Fig. 3. Thermal responses of photosynthetic enzyme activities in eight C_4 grasses. (A–C) Rubisco activity, (D–F) PEPC activity, and (G–I) the PEPC/Rubisco activity ratio as a function of temperature for the C_4 subtypes NADP-ME, PEP-CK, and NAD-ME (as indicated). For each extract, the temperature responses of both enzymes were measured at 18, 25, 34, and 40 °C. Data in (A–F) are fitted according to June *et al.* (2004) and the derived parameters are shown in Table 2. Values are means of 3–4 replicates ±SE.

both 18 and 34 °C. Generally, most leakiness values ranged between 35% at 18 °C and 10% at 40 °C (Supplementary Fig. S11). The estimated C_4 cycle rate (V_p) increased between 18 and 35 °C and was similar between 35 and 40 °C for all the species (Fig. 4D–F, Supplementary Table S1).

Relationships among photosynthetic parameters

In vivo estimates of CO_2 assimilation rate (A), stomatal conductance (g_s), CO_2-saturated rate (CSR), initial slope (IS), and leakiness (ϕ), and *in vitro* measurements of V_{cmax} and V_{pmax} were used to assess how *in vivo* and *in vitro* photosynthetic parameters correlated with short-term changes in temperature.

Weak relationships were observed between IS and V_{pmax} (r^2=0.21, Fig. 5A) and between CSR and V_{cmax} (r^2=0.48, Fig. 5B), and a strong relationship was observed between A and g_s (r^2=0.78, Supplementary Fig. S10). Leakiness (ϕ) was neither correlated to V_{pmax}/V_{cmax} nor to IS/CSR (Fig. 6A, B). The ratios of IS/CSR and V_{pmax}/V_{cmax} were also not correlated (Fig. 6C).

To shed further light on what controls IS in diverse C_4 grasses, we used the simplified expression linking V_{pmax} with IS derived by Pfeffer and Peisker (1998):

$$\text{PEPC activity} = \frac{K_p \cdot \text{IS} \cdot g_m}{g_m - \text{IS}} \quad (12)$$

where K_p is the Michaelis–Menten constant for CO_2. A weak fit was observed between measured V_{pmax} values and model predictions when published K_p values from *Z. mays* were used (Supplementary Fig. S12A, dotted and dashed lines). When equation (12) was solved to simultaneously predict g_m and K_p using measured V_{pmax} and IS values for *Z. mays* at all four temperatures together with published temperature dependencies of g_m and K_p (Bauwe, 1986; Boyd *et al.*, 2015;

Table 2. *Summary of thermal responses of photosynthetic parameters for eight C_4 grasses.*

Coefficients are derived by fitting equation (10) (modified Arrhenius) and equation (11) (June *et al.*, 2004). E_a is the activation energy (kJ mol^{-1}), ΔS is an entropy term (kJ mol^{-1}), k_{25} and P_{opt} are the parameter values at 25 °C and its optimum temperature (T_{opt}), respectively. Ω (°C) is the difference in temperature from T_{opt} at which the parameter falls to e^{-1} (0.37) of its value at T_{opt}. Values are means of three replicates ±SE. The ranking (from lowest =a) of species/subtypes within each individual row was derived using a multiple-comparison Tukey's post hoc test. Values followed by the same letter are not significantly different at the 5% level. *P*-values show significance levels derived by fitting a linear model for all the C_4 species and a linear mixed-effect model for the three C_4 subtypes for each parameter: ns, not significant (P>0.05); * P<0.05; ** P<0.01; *** P<0.001.

Parameter	Const.	NADP-ME			PEP-CK			NAD-ME		Subtype			*P*-value	
		C. ciliaris	*S. bicolor*	*Z. mays*	*M.maximus*	*Ch.gayana*	*E.meyeriana*	*P.coloratum*	*L. fusca*	NADP-ME	PEP-CK	NAD-ME	Species	Subtype
CO_2	E_a	36 ± 1a	42 ± 7a	34 ± 3a	50 ± 7a	36 ± 7a	48 ± 7a	51 ± 4a	54 ± 13a	37 ± 3a	45 ± 4ab	52 ± 5b	ns	*
assimilation	ΔS	0.63 ± 0a	0.63 ± 0a	0.64 ± 0a	0.64 ± 0a	0.63 ± 0.01a	0.63 ± 0a	0.63 ± 0a	0.64 ± 0.01a	0.63 ± 0a	0.63 ± 0a	0.64 ± 0a	ns	ns
rate, *A*	k_{25}	26 ± 1b	28 ± 1b	34 ± 1c	28 ± 1b	28 ± 1b	24 ± 1ab	21 ± 1a	25 ± 0ab	29 ± 1a	27 ± 1a	23 ± 1a	***	0.1
(μmol m^{-2} s^{-1})	P_{opt}	40 ± 1abc	42 ± 0bc	43 ± 1bc	41 ± 1abc	38 ± 1ab	46 ± 3c	36 ± 1a	41 ± 0abc	42 ± 1a	41 ± 1a	38 ± 1a	**	ns
	T_{opt}	41 ± 3a	39 ± 4a	33 ± 1a	35 ± 1a	37 ± 3a	43 ± 6a	39 ± 2a	38 ± 3a	38 ± 2a	38 ± 2a	38 ± 1a	ns	ns
	Ω	25 ± 3a	24 ± 6a	20 ± 2a	18 ± 2a	23 ± 4a	22 ± 5a	20 ± 2a	19 ± 4a	23 ± 2a	21 ± 2a	20 ± 2a	ns	ns
CO_2 saturated	E_a	36 ± 1a	58 ± 2b	45 ± 1ab	45 ± 7ab	42 ± 5ab	49 ± 7ab	44 ± 2ab	37 ± 0ab	47 ± 3a	45 ± 3a	41 ± 2a	*	ns
rate, CSR	ΔS	0.63 ± 0a	0.64 ± 0b	0.64 ± 0b	0.64 ± 0b	0.63 ± 0ab	0.64 ± 0b	0.64 ± 0b	0.63 ± 0ab	0.64 ± 0a	0.64 ± 0a	0.64 ± 0a	**	ns
(μmol m^{-2} s^{-1})	k_{25}	31 ± 1ab	29 ± 1a	34 ± 0b	28 ± 0a	31 ± 1ab	32 ± 1ab	29 ± 1a	30 ± 1ab	32 ± 1a	30 ± 1a	29 ± 1a	ns	ns
	P_{opt}	51 ± 1c	50 ± 1bc	44 ± 1abc	40 ± 2a	45 ± 1ac	49 ± 2bc	42 ± 1a	43 ± 2ab	48 ± 1a	45 ± 1a	42 ± 1a	***	ns
	T_{opt}	42 ± 3b	36 ± 0ab	32 ± 0a	36 ± 0ab	36 ± 1ab	36 ± 1ab	35 ± 0a	36 ± 1ab	37 ± 2a	36 ± 0a	35 ± 0a	**	ns
	Ω	26 ± 3c	17 ± 0bc	17 ± 0ac	21 ± 2a	20 ± 2ac	19 ± 2bc	18 ± 0a	21 ± 1ab	20 ± 2a	20 ± 1a	19 ± 1a	*	ns
Rubisco	E_a	42 ± 3ab	36 ± 6a	52 ± 6ab	38 ± 1ab	52 ± 4ab	42 ± 5ab	47 ± 3ab	58 ± 4b	43 ± 3a	44 ± 3a	52 ± 3a	*	ns
activity, V_{cmax}	ΔS	0.63 ± 0a	0.62 ± 0a	0.63 ± 0a	0.63 ± 0a	0.63 ± 0a	0.63 ± 0a	0.63 ± 0a	0.63 ± 0a	0.63 ± 0a	0.63 ± 0a	0.63 ± 0a	ns	ns
(umol m^{-2} s^{-1})	k_{25}	13 ± 2a	27 ± 3b	27 ± 1b	19 ± 1ab	21 ± 2ab	16 ± 1a	19 ± 1ab	17 ± 1a	23 ± 3a	19 ± 1a	18 ± 1a	***	ns
	P_{opt}	24 ± 4a	47 ± 1b	49 ± 2b	37 ± 3ab	44 ± 3ab	30 ± 3ab	35 ± 6ab	39 ± 7ab	40 ± 4a	37 ± 3a	37 ± 4a	**	ns
	T_{opt}	42 ± 4a	45 ± 2a	39 ± 0a	47 ± 3a	44 ± 4a	46 ± 1a	42 ± 4a	44 ± 4a	42 ± 2a	46 ± 2a	43 ± 3a	ns	ns
	Ω	23 ± 3a	28 ± 2b	20 ± 1b	29 ± 2ab	23 ± 3ab	27 ± 2ab	22 ± 2ab	22 ± 3ab	24 ± 2a	26 ± 1a	22 ± 2a	ns	ns
Initial slope, IS	E_a	47 ± 2ab	70 ± 9b	34 ± 13a	27 ± 3a	48 ± 5ab	43 ± 7ab	47 ± 3ab	52 ± 8ab	53 ± 8a	39 ± 4a	49 ± 3a	**	ns
(μmol m^{-2} s^{-1}	ΔS	0.62 ± 0.01a	0.63 ± 0.01a	0.63 ± 0.01a	0.63 ± 0a	0.64 ± 0a	0.63 ± 0.01a	0.63 ± 0a	0.64 ± 0a	0.63 ± 0a	0.63 ± 0a	0.64 ± 0a	ns	0.06
μbar^{-1})	k_{25}	0.35 ± 0.05ac	0.27 ± 0.04a	0.57 ± 0.02d	0.32 ± 0.02ac	0.41 ± 0.04bc	0.3 ± 0.02ab	0.29 ± 0.01ab	0.47 ± 0.01cd	0.38 ± 0.05a	0.35 ± 0.02a	0.36 ± 0.04a	***	ns
	P_{opt}	1.67 ± 0.68b	0.9 ± 0.1ab	0.73 ± 0.01a	0.42 ± 0.03a	0.63 ± 0.03a	0.66 ± 0.11a	0.49 ± 0.04a	0.7 ± 0.08ab	1.03 ± 0.2a	0.58 ± 0.06a	0.57 ± 0.05a	*	ns
	T_{opt}	72 ± 14b	48 ± 5ab	33 ± 2a	38 ± 2a	36 ± 2a	51 ± 8ab	40 ± 2a	34 ± 2a	49 ± 7a	38 ± 2a	42 ± 3a	**	ns
	Ω	39 ± 4b	22 ± 3ab	20 ± 3a	28 ± 4ab	19 ± 2a	31 ± 5ab	22 ± 2ab	17 ± 0a	25 ± 3a	20 ± 2a	26 ± 3a	*	ns
PEPC activity,	E_a	39 ± 1a	44 ± 3a	61 ± 6bc	39 ± 5a	47 ± 2ab	39 ± 1a	65 ± 3c	51 ± 2ac	48 ± 4a	42 ± 2a	58 ± 4a	***	ns
V_{pmax}	ΔS	0.62 ± 0a	0.64 ± 0cd	0.64 ± 0d	0.63 ± 0bc	0.63 ± 0bd	0.62 ± 0ab	0.64 ± 0cd	0.64 ± 0 cd	0.63 ± 0a	0.63 ± 0a	0.64 ± 0a	***	ns
(μmol m^{-2} s^{-1})	k_{25}	71 ± 6a	186 ± 6c	156 ± 7bc	44 ± 18a	81 ± 12a	135 ± 11b	42 ± 3a	37 ± 7a	138 ± 17a	87 ± 15a	40 ± 4a	***	0.07
	P_{opt}	197 ± 19bcd	255 ± 23d	234 ± 18cd	70 ± 30a	138 ± 23ac	288 ± 33d	90 ± 10ab	61 ± 14a	229 ± 13a	165 ± 35a	76 ± 10a	***	0.07
	T_{opt}	61 ± 5c	33 ± 1a	34 ± 1a	40 ± 1ab	40 ± 2ab	51 ± 3bc	40 ± 3ab	37 ± 1a	43 ± 5a	43 ± 2a	39 ± 2a	***	ns
	Ω	36 ± 2bcd	17 ± 0d	16 ± 1cd	24 ± 3a	21 ± 1ac	30 ± 2d	18 ± 2ab	19 ± 0a	23 ± 3a	25 ± 2a	19 ± 1a	***	ns

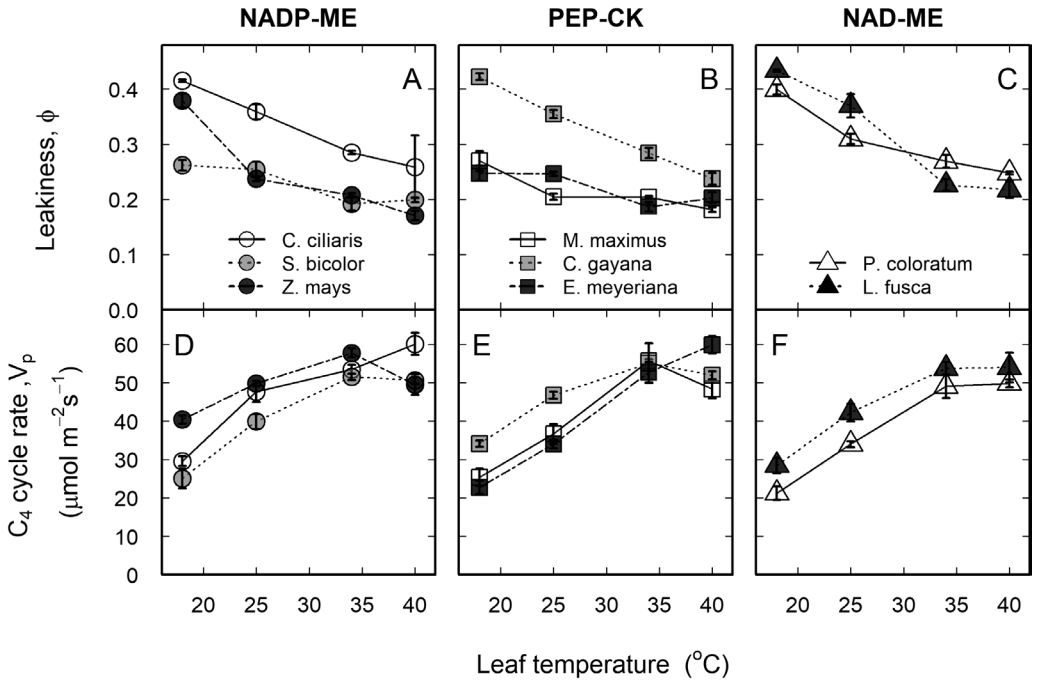

Fig. 4. Thermal responses of bundle sheath leakiness and the C_4 cycle rate in eight C_4 grasses. (A–C) Estimated leakiness (ϕ) and (D–F) C_4 cycle rate (V_p) as a function of leaf temperature for the C_4 subtypes NADP-ME, PEP-CK, and NAD-ME (as indicated). The grasses were grown in a common glasshouse. Leaves were measured at 1800 µmol m^{-2} s^{-1} PPFD and 400 µl l^{-1} CO_2. Values are means of 3–4 replicates ±SE.

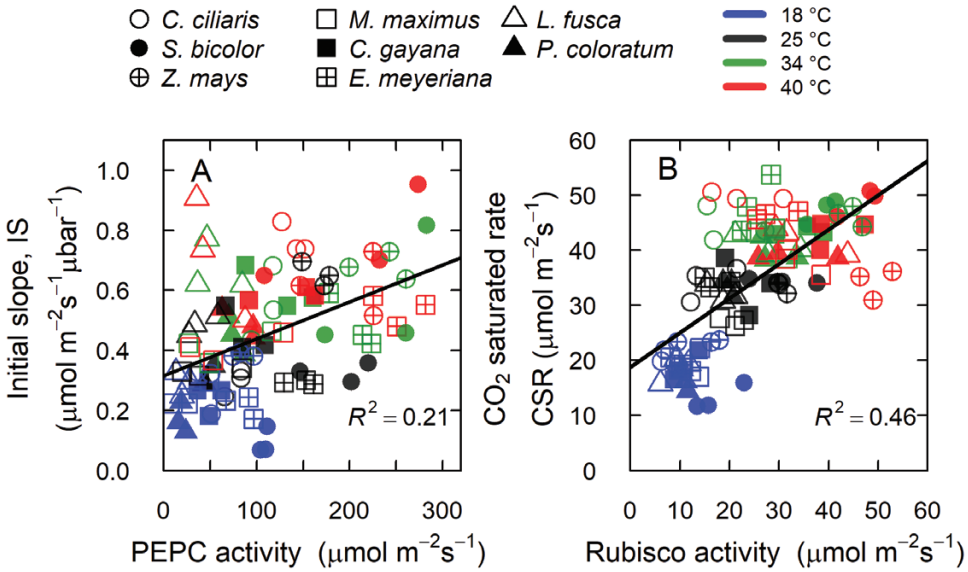

Fig. 5. Relationships between measured *in vitro* and *in vivo* estimates of photosynthetic carboxylases. (A) The initial slope of the CO_2 response curve, IS, versus PEPC activity, and (B) CO_2 saturated rate, CSR, versus Rubisco activity, measured at 18, 25, 34, and 40 °C (as indicated) in the C_4 subtypes NADP-ME (circles), PEP-CK (squares), and NAD-ME (triangles). The solid lines represent regressions of all data points.

Ubierna *et al.*, 2017), the observed fit between the measured and modelled data was much improved (Supplementary Fig. S12A, continuous line, and S12B). Fitted values for *Z. mays* at 25 °C for g_m and K_p were then found to be 1.1 mol m^{-2} s^{-1} and 115 µbar, respectively (Fig. S12A).

Discussion

This study analysed the thermal photosynthetic responses of eight diverse C_4 grasses, deriving constants for thermal dependency that can be incorporated in the C_4 photosynthesis model (von Caemmerer, 2000). The main aim of the study was to determine whether the C_4 biochemical subtype influenced the thermal responses of *in vitro* (V_{pmax} and V_{cmax}) and *in vivo* (IS, CSR, and ϕ) photosynthetic parameters that influence the efficiency of the C_4 CO_2-concentrating mechanism (CCM). The study also explored whether the ratios of IS/CSR and V_{pmax}/V_{cmax} were correlated with each other or with leakiness across a range of C_4 species. The answers to these questions were largely negative, as discussed below.

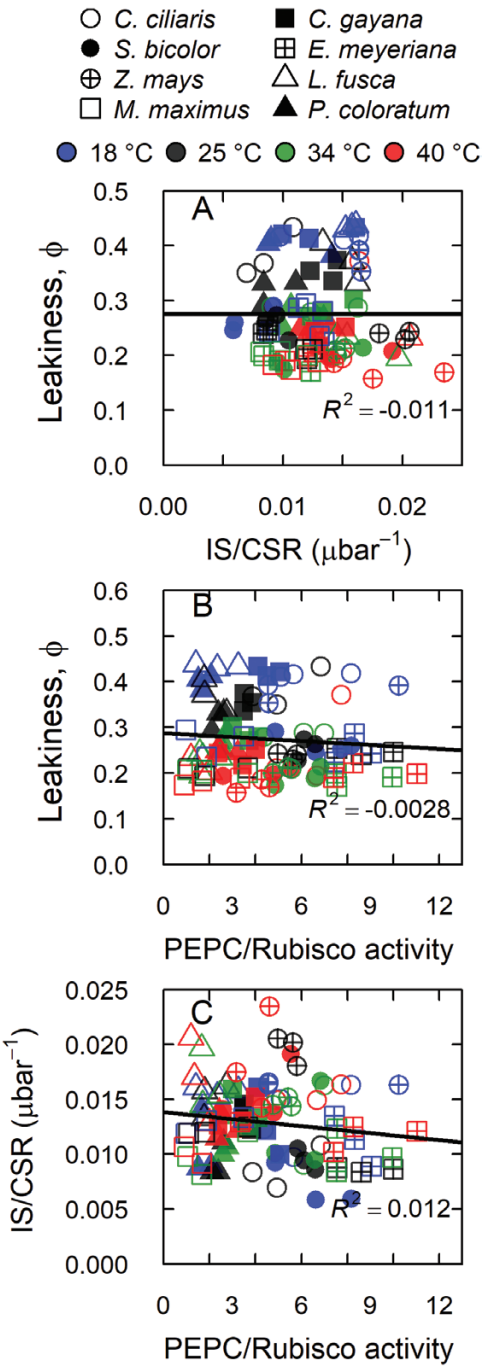

Fig. 6. Relationships between leakiness and the activity ratio of *in vitro* or *in vivo* C_4 and C_3 cycle carboxylases. (A) Leakiness (ϕ) versus the ratio of the initial slope of the CO_2 response curve (IS) and the CO_2-saturated rate (CSR), (B) ϕ versus the ratio of PEPC and Rubisco activities, and (C) the IS/CSR ratio versus the ratio of PEPC and Rubisco activities, measured at 18, 25, 34, and 40 °C (as indicated) in the C_4 subtypes NADP-ME (circles), PEP-CK (squares), and NAD-ME (triangles). The solid lines represent linear regressions of all data points.

Thermal photosynthetic responses varied among the C_4 grasses independently of the biochemical subtype

This study revealed large interspecific variations for most parameters derived from the photosynthetic temperature responses; however, these variations were largely independent of the C_4 subtype, disagreeing with our prediction (Table 2). There was one exception to this generalization, with the activation energy (E_a) of CO_2 assimilation being lowest in the NADP-ME subtype. In addition, V_{pmax} at 25 °C (k_{25}) and at T_{opt} (P_{opt}) were marginally (P=0.07) lowest in NAD-ME and highest in NADP-ME subtypes. The latter observation is consistent with our previous reports of NAD-ME subtypes generally having lower V_{pmax} and V_{pmax}/V_{cmax} (Pinto *et al.*, 2016).

The E_a for *in vitro* V_{cmax} (36–58 kJ mol^{-1}) and V_{pmax} (39–65 kJ mol^{-1}) and their corresponding *in vivo* CSR (36–58 kJ mol^{-1}) and IS (27–70 kJ mol^{-1}) varied by 2-fold among the species examined here. Although these values are in line with published estimates for C_3 (V_{cmax}) and C_4 (V_{cmax} and V_{pmax}) species, they tended to lie at the lower end of the spectrum reported for most of the C_4 grasses used in our study (Ishii *et al.*, 1977; Bernacchi *et al.*, 2001; Medlyn *et al.*, 2002; Sage, 2002; Galmés *et al.*, 2005, 2015; Massad *et al.*, 2007; Walker *et al.*, 2013; Perdomo *et al.*, 2015; Sharwood *et al.*, 2016*a*). For example, higher E_a was reported for V_{cmax} (78 kJ mol^{-1}) and V_{pmax} (95 kJ mol^{-1}) activities in the NADP-ME grass *Setaria viridis* (Boyd *et al.*, 2015), while relatively higher values of E_a were reported for the *in vivo* V_{pmax} of the C_4 species *Z. mays* and *Andropogon gerardii* (60–77.9 kJ mol^{-1}) (Wu and Wedding, 1987; Chen *et al.*, 1994). Interestingly, E_a was higher for V_{cmax} than V_{pmax} in *C. ciliaris*, *Ch. gayana*, *E. meyeriana*, and *L. fusca*, while the opposite was observed in *S. bicolor*, *Z. mays*, *M. maximus*, and *P. coloratum*. Similarly, lower E_a for V_{cmax} than V_{pmax} was reported in *S. viridis* (*in vitro*) (Boyd *et al.*, 2015), and the opposite trend was reported in *A. gerardii* (*in vivo*) (Chen *et al.*, 1994).

We predicted that thermal photosynthetic responses including leakiness may depend on the biochemical subtypes, based on known differences in Rubisco catalytic properties, PSII activity in the BSCs, suberization of the BSC walls, and possibly other anatomical and biochemical traits. In this study, similar thermal responses for leakiness were observed between the C_4 subtypes, and ϕ at 40 °C was similar for all the species. Comparable results were obtained in an earlier study using a smaller set of C_4 grasses measured at a common temperature (Cousins *et al.*, 2008). These results suggest that CCM efficiency is similar among the C_4 subtypes despite their biochemical and anatomical differences. This was evident despite the potential for increased oxygenation in NAD-ME and PEP-CK species with increases in temperature (Siebke *et al.*, 2003) as a result of significant PSII activity in the BSCs of these two subtypes (Edwards *et al.*, 1976; Ghannoum *et al.*, 2005). It has also been suggested that the absence of suberin in the BSC walls of NAD-ME subtypes is counterbalanced by the greater cytosolic barrier that exists for CO_2 diffusion through the centripetal arrangement of BSC chloroplasts surrounded by mitochondria towards the vascular bundle side (von Caemmerer and Furbank, 2003). However, little is known about the thermal dependence of the CO_2 diffusion path from the BSCs to MCs in the different C_4 subtypes.

In the current study, leakiness tended to be higher at the two lowest (18 and 25 °C) relative to the two highest (34 and 40 °C) temperatures for four out of the eight C_4 grasses (see

Supplementary Fig. S11). Similar results were previously reported for a C_4 monocot and a C_4 dicot species (Henderson *et al.*, 1992). To gain further insights about the factors leading to higher leakiness at lower temperatures, we calculated the C_4 cycle rate (V_p). For all the species, the calculated V_p increased with temperature, which indicates that increased leakiness at lower temperatures in some of the species is not related to increased pumping of CO_2 into the BSCs, but is probably due to increased Rubisco limitation. In agreement with this, Sage (2002) showed that C_4 plants are limited by V_{cmax} at low temperature. Taken together, these findings indicate a greater Rubisco limitation at low temperature, which may lead to a greater proportion of CO_2 leakage out of the BSCs in some C_4 species (Kubien *et al.*, 2003; Kubien and Sage, 2004), in a manner not explained by the biochemical subtype.

Maximal in vitro *activities of PEPC and Rubisco, the initial slope and maximal rate of the* A-C_i *curves, and leakiness are not correlated across a range of* C_4 *grasses and leaf temperatures*

Major progress has been made in our understanding of C_3 photosynthesis following the development of a fully mechanistic model (Farquhar *et al.*, 1980) that was subsequently validated by combining leaf gas exchange measurements with estimates of Rubisco activity and mesophyll conductance (g_m) in wild-type (von Caemmerer and Farquhar, 1981; von Caemmerer *et al.*, 1994; Bernacchi *et al.*, 2002; von Caemmerer and Evans, 2015) and genetically altered plants (Hudson *et al.*, 1992). For C_4 photosynthesis, model validation has been undertaken mostly under standard conditions using a genetically altered C_4 dicot, *Flaveria bidentis* (von Caemmerer *et al.*, 1997; Kubien *et al.*, 2003; Pengelly *et al.*, 2012), or under a range of conditions using a limited number of model C_4 grass species, such as *S. bicolor* (Henderson *et al.*, 1992), *Z. mays* (Yin *et al.*, 2016) and *S. viridis* (Boyd *et al.*, 2015). This study presented an ideal opportunity to undertake model validation using *in vitro* enzyme assays and leaf gas exchange measurements for a range of C_4 species.

A weak correlation was observed between CSR and V_{cmax}, while none was found between IS and V_{pmax} (Fig. 5), or between E_a of V_{cmax} (or V_{pmax}) and E_a of CSR (or IS) across the various C_4 grasses. This discrepancy is not surprising and reflects the multitude of factors controlling the A-C_i curves besides the maximal *in vitro* activity of Rubisco and PEPC. Other than Rubisco activity and level of activation, CSR is also dependent on RuBP and PEP regeneration, and both limitations are generally indistinguishable at high light (von Caemmerer, 2000). The IS is determined by the maximal PEPC activity (V_{pmax}), its Michaelis–Menten constant for CO_2 (K_p), and the mesophyll CO_2 partial pressure (C_m), which depends on mesophyll conductance (g_m) (von Caemmerer, 2000). The parameters g_m and K_p were not measured in this study, but using published values at 25 °C together with their temperature dependencies for *Z. mays* (Bauwe, 1986; Boyd *et al.*, 2015; Ubierna *et al.*, 2017) to model the relationship between IS and V_{pmax}, a weak fit was observed between measured and predicted V_{pmax} values (Supplementary Fig. S12A, dotted and dashed lines). In contrast, when model predictions were made using simultaneously solved g_m and K_p values using measured V_{pmax} and IS for *Z. mays* at all four temperatures, the observed fit between measured and modelled V_{pmax} was much improved (Supplementary Fig. S12A, continuous line, and S12B). This exercise indicated that g_m and K_p as well as their temperature responses may vary with growth environment and species (or genotype), as has recently been shown for Rubisco kinetics among these C_4 grasses (Sharwood *et al.*, 2016*a*). The variation in g_m and its temperature response in C_3 species is well established (von Caemmerer and Evans, 2015), and discrepancies for g_m in C_4 *Z. mays* have been reported (Barbour *et al.*, 2016; Ubierna *et al.*, 2017).

In C_3 species, IS (Rubisco-limited photosynthesis) is largely insensitive to temperature because both the K_m and V_{cmax} of Rubisco have a Q_{10} of 2 (Berry and Raison, 1981; Sage and Sharkey, 1987). In contrast, we observed a strong temperature response of IS (PEPC-limited) for the C_4 species examined, indicating that the E_a for V_{pmax} is greater than the E_a of K_p (Table 2, Fig. 2D–F). A similar trend has been shown in a recent study (Boyd *et al.*, 2015). In addition, variation among C_4 species for the E_a of IS suggests that the ratio between E_a for V_{pmax} and K_p also differs. This has been partly supported by our data in the case of the E_a for V_{pmax} (Table 2, Fig. 3D–F). These findings indicate that there is a significant diversity for PEPC kinetics among C_4 species, and warrants further investigation.

The improved relationship between measured and modelled V_{pmax} relative to that observed between IS and measured V_{pmax} (Supplementary Fig. S12A versus S12B) demonstrates that the C_4 photosynthesis model, when well parameterized, can accurately predict CO_2 assimilation rates at limiting C_i in C_4 leaves. Given the rapidly improving methodologies for measuring the exchange of ^{13}C and ^{18}O stable isotopes that allow us to estimate both g_m and K_p (von Caemmerer *et al.*, 2004; Boyd *et al.*, 2015; Barbour *et al.*, 2016; Ubierna *et al.*, 2017), the C_4 photosynthesis model will form a valuable tool for interpreting leaf gas exchange data for any C_4 species under a wide range of environmental conditions, similarly to what has been widely achieved for C_3 plants. Further parameterization and validation of the C_4 photosynthesis model for diverse C_4 species remains a focus of our current research.

Bundle sheath leakiness (ϕ) depends on g_{bs} and the (C_{bs}–C_m) gradient, which in turn depends on the balance between the activities of PEPC and Rubisco (Henderson *et al.*, 1992; von Caemmerer, 2000). In accordance with model predictions, earlier studies reported a relationship between leakiness and *in vitro* V_{pmax}/V_{cmax} (Ranjith *et al.*, 1995; Saliendra *et al.*, 1996; Meinzer and Zhu, 1998) and *in vivo* IS/CSR (Gong *et al.*, 2017). These studies used a single species (sugarcane or *Cleistogenes squarrosa*) exposed to soil or atmospheric water deficit, and estimated ϕ from the C-isotope composition of leaf dry matter rather than photosynthetic C-isotope discrimination as done here. In the current study, leakiness was neither correlated to *in vitro* V_{pmax}/V_{cmax} nor to IS/CSR when all species and leaf temperatures were considered (Fig. 6). There were three exceptions at the species level: leakiness was positively correlated with V_{pmax}/V_{cmax} (but not with IS/CSR) in *Ch. gayana, L. fusca*,

and *Z. mays* (see Supplementary Figs S13 and S14). Hence, we argue that, in response to short-term changes in leaf temperature, CCM efficiency was balanced by biochemical factors, such as enzyme activity, as well as by physical factors, such as g_{bs} (von Caemmerer, 2000). A contribution by g_m is unlikely because very little influence of g_m on the carbon isotope discrimination (Δ) has been predicted (von Caemmerer *et al.*, 2014).

Conclusions

Modelling thermal photosynthetic responses at the leaf level is critical for predicting canopy-scale gas exchange in response to diurnal and seasonal changes in leaf temperature (Harley and Baldocchi, 1995). Thermal sensitivities of parameters used by the C_4 photosynthesis model are needed to accurately predict CO_2 exchange in response to temperature. The findings from the current study demonstrated that, like C_3 photosynthesis (Bernacchi *et al.*, 2001; Walker *et al.*, 2013), *in vivo* and *in vitro* thermal responses of key photosynthetic parameters (e.g. PEPC and Rubisco activities) differ across C_4 species. Hence, relying on the thermal responses of selected species to model C_4 photosynthesis cannot accurately describe ecosystem responses.

The current study also demonstrated that variations in the thermal responses of leakiness (ϕ) among the C_4 grasses is not aligned with the C_4 subtypes. This indicates that various biochemical and anatomical trade-offs operate to maintain similar CCM efficiencies in the various C_4 biochemical pathways. In addition, no correlations were observed among leakiness, V_{pmax}/V_{cmax}, and IS/CSR across a range of C_4 grasses and leaf temperatures. Hence, more work is needed to characterize the thermal responses of g_m and g_{bs} in diverse C_4 species by combining stable isotope and chlorophyll fluorescence studies (Yin *et al.*, 2016).

Supplementary data

Supplementary data are available at *JXB* online.

Table S1. Summary of leaf gas exchange parameters for eight C_4 grasses.

Table S2. Summary of A-C_i-derived parameters and enzyme activities for eight C_4 grasses.

Table S3. Rubisco and protein content of leaves.

Fig. S1. Light environment in the glasshouse during plant growth.

Fig. S2. Comparison of the June *et al.* (2004) and modified Arrhenius models for temperature response.

Fig. S3. Principle component analysis plots for species of the NADP-ME subtype, and all three C_4 subtypes.

Fig. S4. Photosynthetic CO_2 response curves (A-C_i) measured at four-leaf temperatures in eight C_4 grasses.

Fig. S5. Thermal responses of the CO_2 assimilation rate (A), CO_2-saturated rate (CSR), and initial slope of the A-C_i curve (IS) in eight C_4 grasses fitted using the June *et al.* (2004) model.

Fig. S6. Thermal responses of photosynthetic enzyme activities in eight C_4 grasses fitted using the June *et al.* (2004) model.

Fig. S7. Thermal responses of the CO_2 assimilation rate (A), CO_2-saturated rate (CSR), and initial slope of the A-C_i curve (IS) in eight C_4 grasses fitted using the modified Arrhenius model.

Fig. S8. Thermal responses of photosynthetic enzyme activities in eight C_4 grasses fitted using the modified Arrhenius model.

Fig. S9. Photosynthetic carbon isotope discrimination, Δ, as a function of C_i/C_a measured during the gas exchange for eight C_4 grasses.

Fig. S10. Relationship between CO_2 assimilation rates and stomatal conductance in eight C_4 grasses.

Fig. S11. Thermal response of leakiness in eight C_4 grasses.

Fig. S12. Relationship between measured and modelled PEPC activity at various leaf temperatures in *Z. mays*.

Fig.S13. Relationship between leakiness and ratio of PEPC to Rubisco activity in eight C_4 grasses.

Fig. S14. Relationship between leakiness and ratio of initial slope of A-C_i (IS) to CO_2-saturated rates in eight C_4 grasses.

Acknowledgments

We thank Dr Craig Barton for support with the TDL measurements. BVS was supported by a postgraduate research award funded by the Australian Research Council and the Hawkesbury Institute for the Environment at Western Sydney University. This research was funded by the following grants from the Australian Research Council: DP120101603 (OG, SMW), DE130101760 (RES), and CE140100015 (OG, SvC, SMW).

References

Ashton AR, Burnell JN, Furbank RT, Jenkins CLD, Hatch MD. 1990. Enzymes of C_4 photosynthesis. In: Lea PJ, ed. Methods in Plant Biochemistry, vol. **3**: Academic Press, 39–72.

Atkin OK, Westbeek M, Cambridge ML, Lambers H, Pons TL. 1997. Leaf respiration in light and darkness (a comparison of slow- and fast-growing *Poa* species). Plant Physiology **113,** 961–965.

Barbour MM, Evans JR, Simonin KA, von Caemmerer S. 2016. Online CO_2 and H_2O oxygen isotope fractionation allows estimation of mesophyll conductance in C_4 plants, and reveals that mesophyll conductance decreases as leaves age in both C_4 and C_3 plants. New Phytologist **210,** 875–889.

Bauwe H. 1986. An efficient method for the determination of K_m values for HCO_3^- of phosphoenolpyruvate carboxylase. Planta **169,** 356–360.

Bellasio C, Griffiths H. 2014. The operation of two decarboxylases, transamination, and partitioning of C_4 metabolic processes between mesophyll and bundle sheath cells allows light capture to be balanced for the maize C_4 pathway. Plant Physiology **164,** 466–480.

Bernacchi CJ, Bagley JE, Serbin SP, Ruiz-Vera UM, Rosenthal DM, Vanloocke A. 2013. Modelling C_3 photosynthesis from the chloroplast to the ecosystem. Plant, Cell & Environment **36,** 1641–1657.

Bernacchi CJ, Portis AR, Nakano H, von Caemmerer S, Long SP. 2002. Temperature response of mesophyll conductance. Implications for the determination of Rubisco enzyme kinetics and for limitations to photosynthesis *in vivo*. Plant Physiology **130,** 1992–1998.

Bernacchi CJ, Singsaas EL, Pimentel C, Portis AR, Long SP. 2001. Improved temperature response functions for models of Rubisco-limited photosynthesis. Plant, Cell & Environment **24,** 253–259.

Berry JA, Raison JK. 1981. Responses of macrophytes to temperature. In: Lange OL, Nobel PS, Osmond CB, Ziegler H, eds. Physiological plant ecology I: responses to the physical environment. Berlin, Heidelberg: Springer, 277–338.

Boyd RA, Gandin A, Cousins AB. 2015. Temperature responses of C_4 photosynthesis: biochemical analysis of Rubisco, phosphoenolpyruvate

carboxylase, and carbonic anhydrase in *Setaria viridis*. Plant Physiology **169,** 1850–1861.

Brown RH. 1999. Agronomic implications of C_4 photosynthesis. In: Sage RF, Monson RK, eds. C_4 plant biology. San Diego: Academic Press, 473–507.

Chen D-X, Coughenour MB, Knapp AK, Owensby CE. 1994. Mathematical simulation of C_4 grass photosynthesis in ambient and elevated CO_2. Ecological Modelling **73,** 63–80.

Cousins AB, Badger MR, von Caemmerer S. 2008. C_4 photosynthetic isotope exchange in NAD-ME- and NADP-ME-type grasses. Journal of Experimental Botany **59,** 1695–1703.

Crafts-Brandner SJ, Salvucci ME. 2002. Sensitivity of photosynthesis in a C_4 plant, maize, to heat stress. Plant Physiology **129,** 1773–1780.

Crous KY, Quentin AG, Lin YS, Medlyn BE, Williams DG, Barton CV, Ellsworth DS. 2013. Photosynthesis of temperate *Eucalyptus globulus* trees outside their native range has limited adjustment to elevated CO_2 and climate warming. Global Change Biology **19,** 3790–3807.

Dwyer SA, Ghannoum O, Nicotra A, von Caemmerer S. 2007. High temperature acclimation of C_4 photosynthesis is linked to changes in photosynthetic biochemistry. Plant, Cell & Environment **30,** 53–66.

Edwards GE, Huber SC, Ku SB, Rathnam CKM, Gutierrez M, Mayne BC. 1976. Variation in photochemical activities of C_4 plants in relation to CO_2 fixation. In: Burris RH, Black CC, eds. CO_2 metabolism and plant productivity. Baltimore, London, Tokyo: University Park Press, 83–112.

Ehleringer JR, Monson RK. 1993. Evolutionary and ecological aspects of photosynthetic pathway variation. Annual Review of Ecology and Systematics **24,** 411–439.

Evans JR, Sharkey TD, Berry JA, Farquhar GD. 1986. Carbon isotope discrimination measured concurrently with gas exchange to investigate CO_2 diffusion in leaves of higher plants. Functional Plant Biology **13,** 281–292.

Farquhar GD. 1983. On the nature of carbon isotope discrimination in C_4 species. Functional Plant Biology **10,** 205–226.

Farquhar GD, Cernusak LA. 2012. Ternary effects on the gas exchange of isotopologues of carbon dioxide. Plant, Cell & Environment **35,** 1221–1231.

Farquhar GD, von Caemmerer S, Berry JA. 1980. A biochemical model of photosynthetic CO_2 assimilation in leaves of C 3 species. Planta **149,** 78–90.

Farquhar GD, von Caemmerer S, Berry JA. 2001. Models of photosynthesis. Plant Physiology **125,** 42–45.

Furbank RT. 2011. Evolution of the C_4 photosynthetic mechanism: are there really three C_4 acid decarboxylation types? Journal of Experimental Botany **62,** 3103–3108.

Galmés J, Flexas J, Keys AJ, Cifre J, Mitchell RAC, Madgwick PJ, Haslam RP, Medrano H, Parry MAJ. 2005. Rubisco specificity factor tends to be larger in plant species from drier habitats and in species with persistent leaves. Plant, Cell & Environment **28,** 571–579.

Galmés J, Kapralov MV, Copolovici LO, Hermida-Carrera C, Niinemets Ü. 2015. Temperature responses of the Rubisco maximum carboxylase activity across domains of life: phylogenetic signals, trade-offs, and importance for carbon gain. Photosynthesis Research **123,** 183–201.

Ghannoum O, Evans JR, Chow WS, Andrews TJ, Conroy JP, von Caemmerer S. 2005. Faster Rubisco is the key to superior nitrogen-use efficiency in NADP-malic enzyme relative to NAD-malic enzyme C_4 grasses. Plant Physiology **137,** 638–650.

Ghannoum O, Evans JR, von Caemmerer S. 2011. Nitrogen and water use efficiency of C_4 plants. In: Raghavendra AS, Sage RF, eds. C_4 photosynthesis and related CO_2 concentrating mechanisms. Netherlands: Springer, 129–146.

Gong XY, Schäufele R, Schnyder H. 2017. Bundle-sheath leakiness and intrinsic water use efficiency of a perennial C_4 grass are increased at high vapour pressure deficit during growth. Journal of Experimental Botany **68,** 321–333.

Gutierrez M, Gracen VE, Edwards GE. 1974. Biochemical and cytological relationships in C_4 plants. Planta **119,** 279–300.

Harley PC, Baldocchi DD. 1995. Scaling carbon dioxide and water vapour exchange from leaf to canopy in a deciduous forest. I. Leaf model parametrization. Plant, Cell & Environment **18,** 1146–1156.

Harley PC, Thomas RB, Reynolds JF, Strain BR. 1992. Modelling photosynthesis of cotton grown in elevated CO_2. Plant, Cell & Environment **15,** 271–282.

Hatch MD. 1987. C_4 photosynthesis: a unique blend of modified biochemistry, anatomy and ultrastructure. Biochimica et Biophysica Acta **895,** 81–106.

Hattersley PW. 1992. C_4 photosynthetic pathway variation in grasses (Poaceae): Its significance for arid and semi-arid lands. In: Chapman GP, ed. Desertified grasslands: their biology and management. London: Academic Press, 181–212.

Henderson SA, Caemmerer SV, Farquhar GD. 1992. Short-term measurements of carbon isotope discrimination in several C_4 species. Functional Plant Biology **19,** 263–285.

Hudson GS, Evans JR, von Caemmerer S, Arvidsson YB, Andrews TJ. 1992. Reduction of ribulose-1,5-bisphosphate carboxylase/oxygenase content by antisense RNA reduces photosynthesis in transgenic tobacco plants. Plant Physiology **98,** 294–302.

Ishii R, Ohsugi R, Murata Y. 1977. The effect of temperature on the rates of photosynthesis, respiration and the activity of RuDP carboxylase in barley, rice and maize leaves. Japanese Journal of Crop Science **46,** 516–523.

Jenkins CL, Burnell JN, Hatch MD. 1987. Form of inorganic carbon involved as a product and as an inhibitor of C_4 acid decarboxylases operating in C_4 photosynthesis. Plant Physiology **85,** 952–957.

June T, Evans JR, Farquhar GD. 2004. A simple new equation for the reversible temperature dependence of photosynthetic electron transport: a study on soybean leaf. Functional Plant Biology **31,** 275–283.

Kanai R, Edwards GE. 1999. The biochemistry of C_4 photosynthesis. In: Sage RF, Monson RK, eds. C_4 plant biology. San Diego: Academic Press, 49–87.

Kingston-Smith AH, Harbinson J, Foyer CH. 1999. Acclimation of photosynthesis, H_2O_2 content and antioxidants in maize (*Zea mays*) grown at sub-optimal temperatures. Plant, Cell & Environment **22,** 1071–1083.

Kubien DS, Sage RF. 2004. Dynamic photo-inhibition and carbon gain in a C_4 and a C_3 grass native to high latitudes. Plant, Cell & Environment **27,** 1424–1435.

Kubien DS, von Caemmerer S, Furbank RT, Sage RF. 2003. C_4 photosynthesis at low temperature. A study using transgenic plants with reduced amounts of Rubisco. Plant Physiology **132,** 1577–1585.

Leegood RC, Walker RP. 2003. Regulation and roles of phosphoenolpyruvate carboxykinase in plants. Archives of Biochemistry and Biophysics **414,** 204–210.

Lloyd J, Farquhar GD. 1994. ^{13}C discrimination during CO_2 assimilation by the terrestrial biosphere. Oecologia **99,** 201–215.

Massad RS, Tuzet A, Bethenod O. 2007. The effect of temperature on C_4-type leaf photosynthesis parameters. Plant, Cell & Environment **30,** 1191–1204.

Medlyn BE, Dreyer E, Ellsworth D, *et al*. 2002. Temperature response of parameters of a biochemically based model of photosynthesis. II. A review of experimental data. Plant, Cell & Environment **25,** 1167–1179.

Meinzer FC, Zhu J. 1998. Nitrogen stress reduces the efficiency of the C_4 CO_2 concentrating system, and therefore quantum yield, in *Saccharum* (sugarcane) species. Journal of Experimental Botany **49,** 1227–1234.

Pengelly JJ, Sirault XR, Tazoe Y, Evans JR, Furbank RT, von Caemmerer S. 2010. Growth of the C_4 dicot *Flaveria bidentis*: photosynthetic acclimation to low light through shifts in leaf anatomy and biochemistry. Journal of Experimental Botany **61,** 4109–4122.

Pengelly JJ, Tan J, Furbank RT, von Caemmerer S. 2012. Antisense reduction of NADP-malic enzyme in *Flaveria bidentis* reduces flow of CO_2 through the C_4 cycle. Plant Physiology **160,** 1070–1080.

Perdomo JA, Cavanagh AP, Kubien DS, Galmés J. 2015. Temperature dependence of *in vitro* Rubisco kinetics in species of *Flaveria* with different photosynthetic mechanisms. Photosynthesis Research **124,** 67–75.

Pfeffer M, Peisker M. 1998. CO_2 gas exchange and phosphoenolpyruvate carboxylase activity in leaves of *Zea mays* L. Photosynthesis Research **58,** 281–291.

Pinto H, Powell JR, Sharwood RE, Tissue DT, Ghannoum O. 2016. Variations in nitrogen use efficiency reflect the biochemical subtype while variations in water use efficiency reflect the evolutionary lineage of C4 grasses at inter-glacial CO_2. Plant, Cell & Environment **39,** 514–526.

Pittermann J, Sage RF. 2000. Photosynthetic performance at low temperature of *Bouteloua gracilis* Lag., a high-altitude C_4 grass from the Rocky Mountains, USA. Plant, Cell & Environment **23,** 811–823.

R Development Core Team. 2015. R: A language and environment for statistical computing. Vienna, Austria: R Foundation for Statistical Computing, www.r-project.org.

Ranjith S, Meinzer F, Perry M, Thom M. 1995. Partitioning of carboxylase activity in nitrogen-stressed sugarcane and its relationship to bundle sheath leakiness to CO_2, photosynthesis and carbon isotope discrimination. Functional Plant Biology **22,** 903–911.

Sage RF. 2002. Variation in the k_{cat} of Rubisco in C_3 and C_4 plants and some implications for photosynthetic performance at high and low temperature. Journal of Experimental Botany **53,** 609–620.

Sage RF, Peixoto MM, Sage TL. 2013. Photosynthesis in sugarcane. In: Moore PH, Botha FC, eds. Sugarcane: physiology, biochemistry, and functional biology. John Wiley & Sons Ltd, 121–154.

Sage RF, Sharkey TD. 1987. The effect of temperature on the occurrence of O_2 and CO_2 insensitive photosynthesis in field grown plants. Plant Physiology **84,** 658–664.

Saliendra NZ, Meinzer FC, Perry M, Thom M. 1996. Associations between partitioning of carboxylase activity and bundle sheath leakiness to CO_2, carbon isotope discrimination, photosynthesis, and growth in sugarcane. Journal of Experimental Botany **47,** 907–914.

Sharwood RE, Ghannoum O, Kapralov MV, Gunn LH, Whitney SM. 2016a. Temperature responses of Rubisco from Paniceae grasses provide opportunities for improving C_3 photosynthesis. Nature Plants **2,** 16186.

Sharwood RE, Sonawane BV, Ghannoum O. 2014. Photosynthetic flexibility in maize exposed to salinity and shade. Journal of Experimental Botany **65,** 3715–3724.

Sharwood RE, Sonawane BV, Ghannoum O, Whitney SM. 2016b. Improved analysis of C_4 and C_3 photosynthesis via refined *in vitro* assays of their carbon fixation biochemistry. Journal of Experimental Botany **67,** 3137–3148.

Sharwood RE, von Caemmerer S, Maliga P, Whitney SM. 2008. The catalytic properties of hybrid Rubisco comprising tobacco small and sunflower large subunits mirror the kinetically equivalent source Rubiscos and can support tobacco growth. Plant Physiology **146,** 83–96.

Siebke K, Ghannoum O, Conroy JP, Badger MR, von Caemmerer S. 2003. Photosynthetic oxygen exchange in C_4 grasses: the role of oxygen as electron acceptor. Plant, Cell & Environment **26,** 1963–1972.

Tazoe Y, Hanba YT, Furumoto T, Noguchi K, Terashima I. 2008. Relationships between quantum yield for CO_2 assimilation, activity of key enzymes and CO_2 leakiness in *Amaranthus cruentus*, a C_4 dicot, grown in high or low light. Plant & Cell Physiology **49,** 19–29.

Tieszen LL, Sigurdson DC. 1973. Effect of temperature on carboxylase activity and stability in some Calvin cycle grasses from the arctic. Arctic and Alpine Research **5,** 59–66.

Ubierna N, Gandin A, Boyd RA, Cousins AB. 2017. Temperature response of mesophyll conductance in three C_4 species calculated with two methods: ^{18}O discrimination and in vitro V_{pmax}. New Phytologist **214,** 66–80.

Ubierna N, Sun W, Kramer DM, Cousins AB. 2013. The efficiency of C_4 photosynthesis under low light conditions in *Zea mays*, *Miscanthus* × *giganteus* and *Flaveria bidentis*. Plant, Cell & Environment **36,** 365–381.

von Caemmerer S. 2000. Biochemical models of leaf photosynthesis. Collingwood, Australia: CSIRO Publishing.

von Caemmerer S, Evans JR. 2015. Temperature responses of mesophyll conductance differ greatly between species. Plant, Cell & Environment **38,** 629–637.

von Caemmerer S, Evans JR, Hudson GS, Andrews TJ. 1994. The kinetics of ribulose-1,5-bisphosphate carboxylase/oxygenase *in vivo* inferred from measurements of photosynthesis in leaves of transgenic tobacco. Planta **195,** 88–97.

von Caemmerer S, Farquhar GD. 1981. Some relationships between the biochemistry of photosynthesis and the gas exchange of leaves. Planta **153,** 376–387.

von Caemmerer S, Furbank RT. 1999. Modeling C_4 photosynthesis. In: Sage RF, Monson RK, eds. C_4 plant biology. San Diego: Academic Press, 173–211.

von Caemmerer S, Furbank RT. 2003. The C_4 pathway: an efficient CO_2 pump. Photosynthesis Research **77,** 191–207.

von Caemmerer S, Ghannoum O, Pengelly JJ, Cousins AB. 2014. Carbon isotope discrimination as a tool to explore C_4 photosynthesis. Journal of Experimental Botany **65,** 3459–3470.

von Caemmerer S, Lawson T, Oxborough K, Baker NR, Andrews TJ, Raines CA. 2004. Stomatal conductance does not correlate with photosynthetic capacity in transgenic tobacco with reduced amounts of Rubisco. Journal of Experimental Botany **55,** 1157–1166.

von Caemmerer S, Millgate A, Farquhar GD, Furbank RT. 1997. Reduction of ribulose-1,5-bisphosphate carboxylase/oxygenase by antisense RNA in the C_4 plant *Flaveria bidentis* leads to reduced assimilation rates and increased carbon isotope discrimination. Plant Physiology **113,** 469–477.

Walker B, Ariza LS, Kaines S, Badger MR, Cousins AB. 2013. Temperature response of *in vivo* Rubisco kinetics and mesophyll conductance in *Arabidopsis thaliana*: comparisons to *Nicotiana tabacum*. Plant, Cell & Environment **36,** 2108–2119.

Wang Y, Bräutigam A, Weber AP, Zhu XG. 2014. Three distinct biochemical subtypes of C_4 photosynthesis? A modelling analysis. Journal of Experimental Botany **65,** 3567–3578.

Wingler A, Walker RP, Chen ZH, Leegood RC. 1999. Phosphoenolpyruvate carboxykinase is involved in the decarboxylation of aspartate in the bundle sheath of maize. Plant Physiology **120,** 539–546.

Wu MX, Wedding RT. 1987. Temperature effects on phosphoenolpyruvate carboxylase from a CAM and a C_4 plant: a comparative study. Plant Physiology **85,** 497–501.

Yin X, van der Putten PE, Driever SM, Struik PC. 2016. Temperature response of bundle-sheath conductance in maize leaves. Journal of Experimental Botany **67,** 2699–2714.